How to Solve the Stochastic Six Vertex Model

Leonid Petrov

At 04:23, on Wednesday 12$^{\text{th}}$ July, 2023

Introduction

These are lecture notes for PANEM-2023 at Texas A&M on the integrability and asymptotics of the stochastic six vertex model.

1 Lecture I. Six vertex model through different lenses

In the first lecture, we describe the stochastic six vertex model from two diverse perspectives — as a model of statistical mechanics, and as a stochastic particle system.

1.1 Gibbs measures and the six vertex model

1.1.1 Finite-volume Gibbs measures

We begin with describing the useful framework of *Gibbs measures*. For simplicity, we work on the two-dimensional lattice $\mathbb{Z}^2$. Let $\Lambda \subset \mathbb{Z}^2$ be a finite subset (for example, a rectangle). We are interested in *spin configurations* inside Λ which are encoded as $\omega = \{\sigma_e \colon e \text{ is an edge in } \Lambda\}$, where $\sigma_e \in \{0, 1\}$. By an "edge in Λ" we mean that both endpoints of this edge must be inside Λ. Each spin configuration is equipped with boundary conditions, which are fixed spins on all the boundary edges of Λ (an edge is called boundary if it connects Λ to $\mathbb{Z}^2 \setminus \Lambda$).

With each spin configuration ω, we associate its energy $H(\omega) \in \mathbb{R}$. This energy may depend on global parameters (e.g., inverse temperature) and local parameters (e.g., edge capacities or vertex rapidities). If a particular spin configuration ω is forbidden, we have $H(\omega) = +\infty$.

Definition 1.1. The (finite-volume) *Gibbs measure* in Λ with fixed boundary conditions and the energy function $H(\cdot)$ is the probability distribution on spin configurations whose probability weights have the form

$$\mathrm{Prob}(\omega) = \frac{1}{Z} \exp\{-H(\omega)\}.$$

Here Z is the *partition function*, which is simply the probability normalizing constant.

For a given finite region, boundary conditions, and the energy function, a Gibbs measure is unique.

Example 1.2 (Domino tilings on the square grid)**.** A *perfect matching* on Λ is any subset M of its edges such that every vertex is covered by exactly one edge from M. For example, here is a perfect matching on the four by four rectangle:

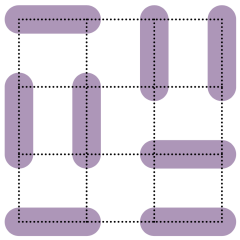

If the set of allowed spin configurations is the set of perfect matchings (with $\sigma_e = 1$ if the edge is included in the matching, and $\sigma_e = 0$ otherwise), and

$$H(\omega) = \begin{cases} 0, & \omega \text{ is a perfect matching;} \\ +\infty, & \omega \text{ is not a perfect matching,} \end{cases}$$

then the corresponding Gibbs measure is the uniform distribution on the space of *domino tilings*. That is, we identify each covered edge with a 2×1 domino. The domino tiling corresponding to the above perfect matching is

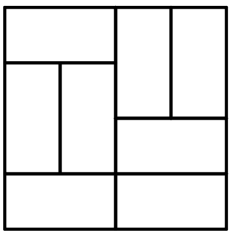

Exercise 1.1. Compute the number of domino tilings of the thin rectangles

(a) $2 \times n$;

(b) $3 \times (2n)$.

Computing partition functions of various Gibbs measures may be challenging. For example, the number of domino tilings of the 8×8 chessboard is 12,988,816, but its theoretical computation (not via a computer program) requires several nontrivial steps [Kas61], [TF61].

Parameter-dependent partition functions represent many important quantities across all of mathematics, including various families of symmetric functions (such as Schur or Hall-Littlewood functions), and related objects.

1.1.2 Infinite-volume Gibbs measures

Besides Gibbs measures on configurations on a finite space as in Definition 1.1 with fixed boundary conditions ("*boxed distributions*"), we are interested in *infinite-volume* Gibbs measures.

Definition 1.3. A probability measure on spin configurations on an infinite subset $\Lambda_\infty \subseteq \mathbb{Z}^2$ (we will mainly consider the whole plane and the quarter plane $\mathbb{Z}^2_{\geq 0}$) is called (infinite-volume) Gibbs if for any finite $\Lambda \subset \Lambda_\infty$, the configuration inside Λ conditioned on the configuration in $\Lambda_\infty \setminus \Lambda$ is a finite-volume Gibbs measure in the sense of Definition 1.1 (with boundary conditions imposed by the outside configuration in $\Lambda_\infty \setminus \Lambda$).

Out of all possible infinite-volume Gibbs measures, we are interested in measures with special properties, such as translation invariant and/or ergodic. A Gibbs measure on $\mathbb{Z}^2$ is called *translation invariant* if its distribution does not change under arbitrary space translations. A Gibbs measure is called *ergodic* (equivalently, *extremal*) if it cannot be represented as a convex combination of two other such measures. Gibbs measures which are translation invariant and ergodic (within the class of translation invariant measures) are called *pure states*.

Classifying pure states for a given energy function $H(\cdot)$ is a very nontrivial problem, and an explicit answer is rarely available. For the general six vertex model (defined in Section 1.1.3 below), the answer is only conjectural [Res10].

On the other hand, pure states of the six vertex model under a special *free fermion condition* (which includes the domino model from Example 1.2) admit a very explicit description through determinantal point processes (i.e., all correlation functions of these measures are diagonal minors

of an explicit function in two variables), which follows from [She05], [KOS06]. One of the goals of these lecture notes is to discuss the tools and results one would require to extend this classification beyond the free fermion case.

Remark 1.4. Certain families of non translation invariant infinite-volume Gibbs measures (under the free fermion condition) power the classification of irreducible representations of infinite-dimensional unitary group and other classical groups [Voi76], [VK82], [BO12], [Pet14]. This subject is closely related to symmetric functions arising as partition functions of Gibbs measures with varying parameters (rapidities) along one of the lattice coordinate direction which we discuss in the second lecture (Section 2). There is also a direct link between these Gibbs measures and totally nonnegative triangular or full Toeplitz matrices for characters of the infinite symmetric group or, respectively, the infinite-dimensional unitary group, see [AESW51], [Edr53], [Boy83].

1.1.3 Six vertex model

The most general Gibbs property we consider in these notes is that of the *asymmetric six vertex model*. The six vertex model was introduced by Pauling to model the residual entropy of ice [Pau35] (see also [ASLW+15] for recent experiments with square ice between two graphene sheets, and Remark 1.5 below for an exact connection). The model has received a lot of attention since the seminal Bethe Ansatz solutions obtained in the 1960's in [Lie67], [YY66]. We refer to the book [Bax07] for an introduction, and also to [Res10], [BH20] for recent surveys of the model and its history, respectively.

Under the asymmetric six vertex model, the allowed spin configurations on the two-dimensional lattice are such that locally around each vertex there can be one of the following six configurations:

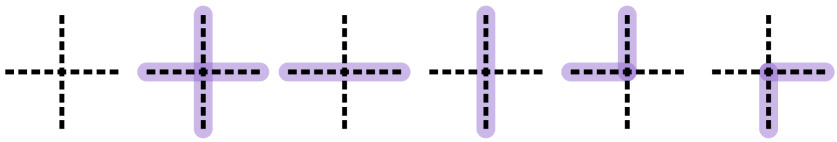

Viewing the edges with spin $\sigma_e = 1$ as parts of up-right paths, we can think of six vertex model configurations as up-right path configurations on the lattice, where paths are allowed to touch at a vertex. We denote the six vertex types by $a_1, a_2, b_1, b_2, c_1, c_2$:

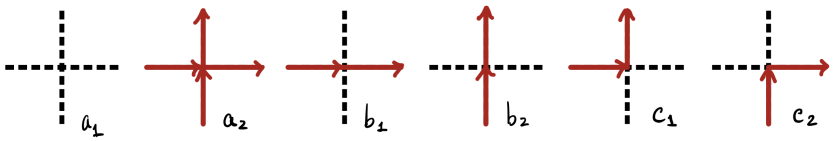

(1.1)

See Figure 1, right, for an example of a global configuration of up-right paths in a rectangle.

Abusing the notation, we also think of $a_1, a_2, b_1, b_2, c_1, c_2 \geq 0$ as the Gibbs weights e^{-H} assigned to each local vertex. That is, the six vertex model Gibbs measure in a rectangle Λ with given boundary conditions (that is, with prescribed spin configurations at all edges connecting Λ to $\mathbb{Z}^2 \setminus \Lambda$) has probability weights

$$\mathrm{Prob}(\omega) = \frac{a_1^{\#\{a_1 \text{ vertices}\}} a_2^{\#\{a_2 \text{ vertices}\}} b_1^{\#\{b_1 \text{ vertices}\}} b_2^{\#\{b_2 \text{ vertices}\}} c_1^{\#\{c_1 \text{ vertices}\}} c_2^{\#\{c_2 \text{ vertices}\}}}{Z(a_1, a_2, b_1, b_2, c_1, c_2)}.$$

Here $\#\{a_1 \text{ vertices}\}$ is the number of vertices of type a_1 in the configuration ω, and so on.

Remark 1.5 (Connection to square ice)**.** In the square ice, the oxygen atoms should form a perfect square grid, and each edge contains a hydrogen atom. The hydrogen atom on an edge is connected to one of the adjacent oxygens by the chemical bond, and to another oxygen by a weaker hydrogen bond. This allows to distinguish two types of edges, and assign "spins" 0 and 1 to them. Since each oxygen must have exactly two hydrogen atoms attached to it by chemical bonds, we get six possible local configurations around a vertex. See Figure 1 for an illustration.

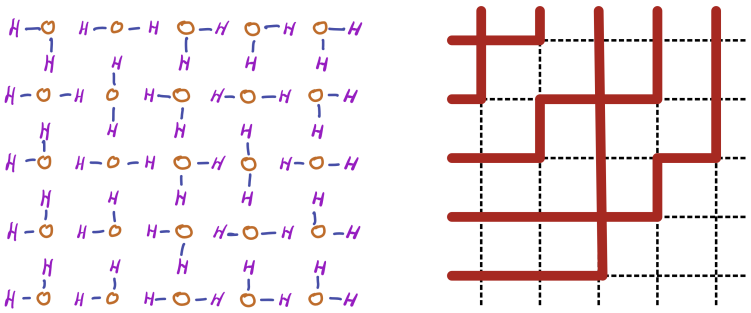

Figure 1: Left: a configuration of the square ice. Right: the corresponding configuration of the six vertex model in the square grid.

The quantity

$$\Delta := \frac{a_1 a_2 + b_1 b_2 - c_1 c_2}{2\sqrt{a_1 a_2 b_1 b_2}} \tag{1.2}$$

plays an important role in the (mostly conjectural) description of pure phases of the asymmetric six vertex model. Depending on Δ, there are several regimes of the model:

- Ferroelectric: $\Delta > 1$;
- Anti-ferroelectric: $\Delta < 1$;
- Disordered: $-1 < \Delta < 1$;
- Free fermion point: $\Delta = 0$.

Example 1.6 (Free fermion specializations)**.** Specializing the weights $a_1, a_2, b_1, b_2, c_1, c_2$ in two different free fermion ways, we obtain the following particular cases:

- If $a_1 = a_2 = b_1 = b_2 = 1$ and $c_1 = c_2 = \sqrt{2}$, one can map six vertex configurations into domino tilings from Example 1.2. This map is not a bijection between configurations, but instead it splits a c-type vertex into two equivalent local configurations of the domino tilings, while preserving the configuration weights. This idea goes back to [EKLP92], see also [ZJ00], [FS06]. A multiparameter generalization of the domino tiling model coming from the free fermion six vertex model was considered in [ABPW21], see also [Nap23].

- When $a_2 = 0$ and $a_1 = b_1 = b_2 = c_1 = c_2 = 1$, we forbid the intersection of paths. This model can be bijectively mapped into a model of *lozenge tilings* (e.g., see [Gor21] for the definition), with configurations like

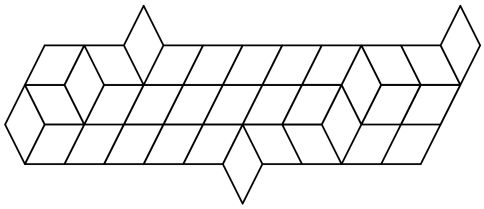

Exercise 1.2. (a) Work out the details of the mapping from the free fermion six vertex model with $a_2 = 0$ and $a_1 = b_1 = b_2 = c_1 = c_2 = 1$ to lozenge tilings. What happens to the boundary conditions?

(b) If we set $b_1 = c_1 = u_x v_y$, where (x, y) are the lattice coordinates of a vertex, then six vertex configurations start depending on the parameters u_i, v_j (which we assume to be generic complex numbers). How do these weights translate into the lozenge tiling picture?

In the next Section 1.2 we consider another important particular case — the *stochastic six vertex model*, which is no longer free fermion.

Remark 1.7 (Alternating sign matrices)**.** There are other very interesting specializations of the six vertex model which are not stochastic nor free fermion. Let us only mention that when $a_1 = a_2 = b_1 = b_2 = c_1 = c_2 = 1$ (so $\Delta = 1/2$, which is in the disordered regime), the six vertex Gibbs property becomes uniform (on configurations of up-right paths which are allowed to touch at a vertex). There is a bijection from six vertex configurations to *alternating sign matrices*. This bijection allowed to compute the number of alternating sign matrices from a partition functions of the six vertex model. We refer to [Kup96] and [Pro01] for details.

1.2 Stochastic six vertex model and its particle system limits

1.2.1 Stochastic six vertex model

Sampling six vertex configurations by Glauber dynamics (which proceeds by random local flips as in (1.8) below) can be exponentially slow under some conditions on the parameters [FR19]. Here we consider a case of parameters under which the sampling (in the case when the top and the right boundaries are "free") can instead be done by running a Markov chain just once.

Definition 1.8. The six vertex model with parameters $a_1, a_2, b_1, b_2, c_1, c_2$ (1.1) is called *stochastic* if

$$a_1 = a_2 = 1, \qquad b_1 + c_1 = b_2 + c_2 = 1, \qquad b_1, b_2 \in [0, 1]. \tag{1.3}$$

The stochastic six vertex model depends on the two remaining parameters (b_1, b_2).

Let us explain how conditions (1.3) simplify the sampling of the model. Take a finite rectangle $\Lambda \subset \mathbb{Z}^2$, and equip it with *free outgoing boundary conditions*, for which the locations of outgoing paths on the right and the top boundaries of the rectangle are not specified. Due to the

stochasticity condition (1.3), the partition function of the stochastic six vertex Gibbs measure in Λ with these boundary conditions is simply equal to 1.

The stochastic six vertex configuration in Λ can be sampled by running a row-to-row Markov chain based on the vertex weights, see Figure 2 for an illustration.

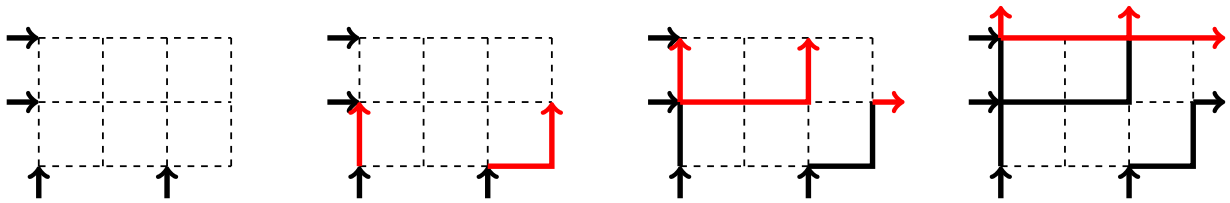

Figure 2: Sampling the configuration of the stochastic six vertex model in a rectangle Λ with free outgoing boundary conditions by the row-to-row Markov chain. At each step, we perform the sequential update (from left to right) in a single row using the incoming paths from the left and from the row below. For example, after one step the probability of getting the displayed configuration is equal to $b_2c_2c_1$.

The stochastic six vertex model was introduced in [GS92]. The stochastic specialization of the parameters allows to study this particular case of the six vertex model using the toolbox from stochastic interacting particle systems [Lig05], by treating the vertical direction as time. In Sections 1.2.3 and 1.2.4 below we consider two limits of the stochastic six vertex model to more familiar continuous time interacting particle systems.

1.2.2 Limit shape

We are now in a position to formulate the limit shape result for the stochastic six vertex model whose proof will be given in Section 3 in the last lecture. This limit shape result was first proven in [BCG16] by adapting the techniques from the ASEP (Asymmetric Simple Exclusion Process) pioneered in [TW08], [TW09]. Our goal in these lecture notes is to present another proof which highlights the use of several other integrability techniques, most importantly, the Yang–Baxter equation and symmetric functions (discussed in the second lecture, Section 2).

Consider the stochastic six vertex model in the quadrant $\mathbb{Z}^2_{\geq 0}$ with the *infinite domain wall* boundary conditions. That is, there are incoming arrows at each edge along the left boundary of the quadrant, and no incoming arrows at the bottom boundary.

The stochastic six vertex model in this infinite domain can be sampled by running a Markov chain as in Figure 2. See Figure 4, right, for an example of a configuration.

Define the height function of the vertex model at the discrete level by

$$H(x,y) \coloneqq \#\{\text{up-right paths to the right of the point } (x,y)\}, \qquad (x,y) \in \mathbb{Z}^2_{\geq 0}. \tag{1.4}$$

See Figure 3 for an example.

Let $b_1 > b_2$ and

$$u \coloneqq \frac{1-b_1}{1-b_2}. \tag{1.5}$$

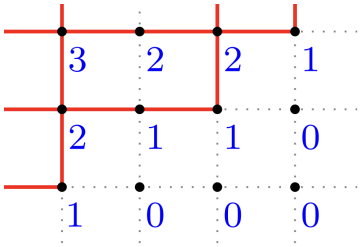

Figure 3: Height function of the stochastic six vertex model with infinite domain wall boundary conditions.

Define the following function on $\mathbb{R}^2_{\geq 0}$:

$$\mathfrak{h}(\mathsf{x},\mathsf{y}) := \begin{cases} \mathsf{y}-\mathsf{x}, & \text{if } \frac{\mathsf{y}}{\mathsf{x}} > \frac{1}{u}; \\ \dfrac{(\sqrt{\mathsf{y}}-\sqrt{u\mathsf{x}})^2}{1-u}, & \text{if } u < \frac{\mathsf{y}}{\mathsf{x}} < \frac{1}{u}; \\ 0, & \text{if } \frac{\mathsf{y}}{\mathsf{x}} < u. \end{cases} \tag{1.6}$$

Theorem 1.9 (Limit shape of the stochastic six vertex model [BCG16])**.** *We have convergence in probability for any* $(\mathsf{x},\mathsf{y}) \in \mathbb{R}^2_{\geq 0}$*:*

$$\lim_{\varepsilon \to 0} \varepsilon H\left(\lfloor \varepsilon^{-1}\mathsf{x} \rfloor, \lfloor \varepsilon^{-1}\mathsf{y} \rfloor\right) = \mathfrak{h}(\mathsf{x},\mathsf{y}),$$

where the limiting height function $\mathfrak{h}$ *is given by* (1.6).

The condition $b_1 > b_2$ in Theorem 1.9 is important, as for $b_1 \leq b_2$ the up-right paths will not travel macroscopically far to the right, and the limit shape function is simply $y - x$ when $y > x$. In the symmetric case $b_1 = b_2$, there should be a limit shape result on the scale $\varepsilon^{-1/2}$ instead of ε^{-1} (for example, see [IMS21] and references therein to related work).

Remark 1.10. Along with Theorem 1.9, we will show that the fluctuations of the height function H around its limit $\mathfrak{h}$ have order $\varepsilon^{-1/3}$, and are given by the GUE Tracy–Widom distribution F_2. This was also obtained in [BCG16]. The GUE Tracy–Widom fluctuations were first observed in random matrix theory [For93], [TW94]. For the stochastic six vertex model, these fluctuations manifest the fact that the model belongs to the *KPZ universality class* named after the seminal work of Kardar–Parisi–Zhang [KPZ86]. See, for example, [Cor12] for a survey on KPZ universality.

1.2.3 Diagonal limit to ASEP

Let us take the limit of the stochastic six vertex model with the infinite domain wall boundary condition as $b_1, b_2 \to 0$, but their ratio $b_2/b_1 = q$ stays fixed. When $b_1 = b_2 = 0$, each up-right path performs a deterministic staircase motion. However, in the limit as $b_1, b_2 \to 0$, as we take a large domain of the size proportional to b_2^{-1}, the staircases will occasionally move "up" or "down".

More precisely, let us view the diagonal direction as the new time axis:

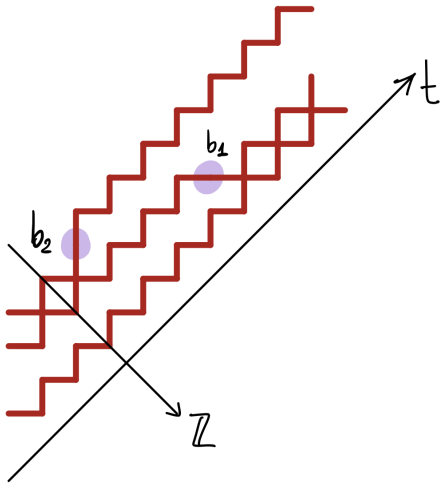

In this picture, we highlighted the two occasional moves, first "up" with probability b_2, and second "down" with probability b_1. In the Poisson type scaling limit when the discrete diagonal time becomes continuous, the staircases may be mapped to interacting particles on the line:

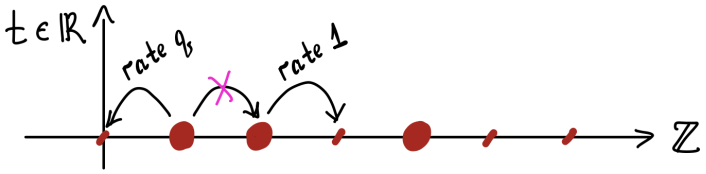

The motion of the particles is as follows. In continuous time, each particle has two independent exponential clocks with rates 1 and q. Clocks of different particles are independent from each other. By "exponential clocks of rate λ" we mean a clocks which rings after an exponential random time T with $\text{Prob}(T > s) = e^{-\lambda s}$. Due to the memorylessness of the exponential distribution, the ringing of one clock does not affect all other clocks. When a clock of rate q or 1 at a particle rings, it jumps left or right by one, respectively, under the condition that the destination is not occupied. If the destination is occupied, the jump is suppressed.

This particle system (Markov process on particle configurations on $\mathbb{Z}$) is called the Asymmetric Simple Exclusion Process, or *ASEP*, for short. It was introduced over 50 years ago in biology [MGP68], [MG69] and probability [Spi70].

In our limit from the stochastic six vertex model, the initial condition for ASEP is the *step initial condition*, under which all negative sites of $\mathbb{Z}$ are occupied. However, ASEP can start from an arbitrary particle configuration on $\mathbb{Z}$, and the existence of the process can be established using Harris' graphical construction [Har78]. In the particular case $q = 0$, ASEP turns into TASEP (Totally Asymmetric Simple Exclusion Process), in which particles jump only to the right.

1.2.4 PushTASEP limit

Let us keep the infinite domain wall boundary condition in the stochastic six vertex model. In another Poisson type limit as $c_1 \to 0$, the up-right paths become very long and horizontal. For simplicity, let us first assume that also $b_2 = 0$. Treating the horizontal axis as the new time, and rescaling this time from discrete to continuous by the factor of c_1^{-1} leads to a particle system which is known as PushTASEP (Pushing Totally Asymmetric Simple Exclusion Process) or long-range TASEP. PushTASEP is a very close relative of TASEP. It was introduced in [Spi70] and studied in a number of papers, including [DLSS91], [DW08], [BF08].

In the PushTASEP limit of the stochastic six vertex model, particles live on $\mathbb{Z}_{\geq 0}$ (which we draw vertical) and jump up in continuous time. Each particle has an independent exponential clock of rate 1. When the clock rings, the particle jumps up by 1, and pushes up by 1 any particle that is in the way:

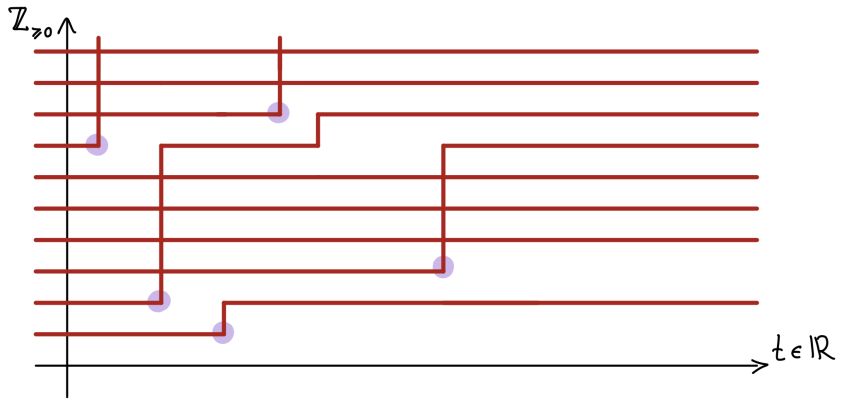

Here we highlighted the rare events which occur with probability $c_1 \to 1$.

Remark 1.11. For the PushTASEP coming from the infinite domain wall boundary condition, in any finite time interval $[0, t)$, infinitely many particles get pushed up to infinity and leave the system. This infinity of jumps in a finite time does not create problems, since the marginal evolution of the PushTASEP restricted to $\{0, 1, 2, \dots, K\} \subset \mathbb{Z}_{\geq 0}$ for any $K \geq 1$ is independent of the rest of the system. Therefore, we can define the evolution of the PushTASEP on the whole lattice $\mathbb{Z}_{\geq 0}$ by Kolmogorov extension.

If we did not set $b_2 = 0$ in the PushTASEP limit, we would get a one-parameter deformation of PushTASEP which is known as the *Hall-Littlewood PushTASEP* [BBW16], [Gho17]. In this deformed process, each jumping particle first jumps up by 1, but then can continue moving up, with probability $q \in [0, 1)$ per each extra step, as long as there are no other particles in the way. When there is a particle in the way, the moving particle stops, but the next particle is activated, and will continue jumping up according to the same mechanism. Here, as before, $q = b_2/b_1$, and recall that $b_1 \to 1$.

Exercise 1.3. Prove the claims made in Remark 1.11, and extend them to the Hall-Littlewood PushTASEP. Is the marginal Markov structure of the PushTASEP preserved under the deformation?

1.3 Gibbs measures from the stochastic six vertex model

The stochastic six vertex model Gibbs property depending on two parameters (b_1, b_2) seems much more restrictive than the Gibbs property of the general six vertex model with all six parameters $(a_1, a_2, b_1, b_2, c_1, c_2)$, see (1.1). However, by renormalizing the vertex weights in a finite region $\Lambda \subset \mathbb{Z}^2$, we may reduce a rather general six vertex model Gibbs property (namely, the symmetric, ferroelectric one) to the stochastic one. This result is due to Aggarwal [Agg18, Appendix A.1] using some of the observations from [BB17]. For convenience, we reproduce the full proof here.

Proposition 1.12. *Let $a_1 = a_2 = \mathcal{A}$, $b_1 = b_2 = \mathcal{B}$, and $c_1 = c_2 = \mathcal{C}$, where $\mathcal{A}, \mathcal{B}, \mathcal{C} \geq 0$ satisfy the ferroelectric condition*

$$\Delta = \frac{\mathcal{A}^2 + \mathcal{B}^2 - \mathcal{C}^2}{2\mathcal{A}\mathcal{B}} > 1$$

and $\mathcal{A} > \mathcal{B}$. Then, in any finite region $\Lambda \subset \mathbb{Z}^2$ with fixed boundary conditions on all sides, the Gibbs measure under the six vertex model with parameters $(a_1, a_2, b_1, b_2, c_1, c_2)$ coincides with the Gibbs measure under the stochastic *six vertex model with parameters $(\tilde{b}_1, \tilde{b}_2)$, where*

$$\tilde{b}_1 = \frac{\mathcal{B}}{\mathcal{A}} \left(\Delta + \sqrt{\Delta^2 - 1} \right), \qquad \tilde{b}_2 = \frac{\mathcal{B}}{\mathcal{A}} \left(\Delta - \sqrt{\Delta^2 - 1} \right). \tag{1.7}$$

The condition $\mathcal{A} > \mathcal{B}$ is not restrictive. Indeed, if $\mathcal{A} = \mathcal{B}$, we cannot have $\Delta > 1$. If $\mathcal{A} < \mathcal{B}$, we can exchange $\mathcal{A}$ and $\mathcal{B}$ by rotating the lattice clockwise by 90 degrees and flipping the spins $\sigma_e \mapsto 1 - \sigma_e$ for each horizontal edge e. Thus, it suffices to assume $\mathcal{A} > \mathcal{B}$.

For $\mathcal{A} > \mathcal{B}$, the condition $\Delta > 1$ is required so that the resulting stochastic six vertex model is an honest probability distribution with real nonnegative probability weights, that is, $\tilde{b}_1, \tilde{b}_2 \in [0, 1]$.

Proof of Proposition 1.12. The argument relies on *conservation laws* which hold in the finite region Λ with fixed boundary conditions. For each given configuration of up-right paths in Λ, denote by $\#_{a_1}, \#_{a_2}, \#_{b_1}, \#_{b_2}, \#_{c_1}, \#_{c_2}$ the number of vertices of the corresponding type in this configuration, see (1.1). Then we have (where *const* stand for quantities which depend only on Λ and the fixed boundary conditions, but not on a particular configuration of up-right paths):

- $\#_{a_1} + \#_{a_2} + \#_{b_1} + \#_{b_2} + \#_{c_1} + \#_{c_2} = const$, because this is the total number of vertices in Λ;
- $\#_{a_2} + \#_{b_2} + \#_{c_1} = const$, because the total number of occupied vertical edges (i.e., with spin 1) is constant, and each vertical edge begins at a vertex of type a_2, b_2, or c_1;
- $\#_{a_2} + \#_{b_1} + \#_{c_2} = const$, by similarly considering occupied horizontal edges;
- $\#_{c_1} - \#_{c_2} = const$, see Exercise 1.5 below for details.
- $\#_{b_1} - \#_{b_2} = const$, which follows from the previous three conservation laws.

Using these conservation laws, one can check that the six vertex Gibbs measures with parameters $(a_1, a_2, b_1, b_2, c_1, c_2)$ and the modified parameters $(wa_1, wa_2, wt^{-1}b_1, wtb_2, w\xi^{-1}c_1, w\xi c_2)$ (where $w, t, \xi > 0$ are arbitrary) are the same. Taking $a_1 = a_2 = \mathcal{A}$, $b_1 = b_2 = \mathcal{B}$, and $c_1 = c_2 = \mathcal{C}$, and

$$w = \mathcal{A}^{-1}, \qquad t = \Delta + \sqrt{\Delta^2 - 1}, \qquad \xi = \frac{\mathcal{A}(1 - \tilde{b}_2)}{\mathcal{C}} = \frac{\mathcal{A} - \mathcal{B}\Delta + \mathcal{B}\sqrt{\Delta^2 - 1}}{\mathcal{C}}$$

makes the modified parameters of the Gibbs measure stochastic, namely, $(1, 1, \tilde{b}_1, \tilde{b}_2, 1 - \tilde{b}_1, 1 - \tilde{b}_2)$. This completes the proof. □

Exercise 1.4. Verify the two claims made before the proof of Proposition 1.12.

Exercise 1.5. (a) Show the conservation law $\#_{c_1} - \#_{c_2} = const$. Argue as follows. First, show that any up-right path configuration in Λ can be related to any other up-right configuration with the same boundary conditions by a sequence of local flips of the form:

(1.8)

Here we change only the configuration of occupied edges along a single lattice square, and do not change any other parts of the configuration (which can be arbitrary outside this single square).

(b) Show that under the flips (1.8), the numbers $\#_{c_1}$ change $\#_{c_2}$ by the same amount, so that their difference stays constant.

By Proposition 1.12, all possible Gibbs measures of the symmetric, ferroelectric six vertex model in a finite volume are obtained by running the stochastic six vertex Markov chain with given initial conditions and conditioned on a given final configuration. By taking limits, this observation allows to study pure states of symmetric, ferroelectric six vertex model by probabilistic techniques. For example, this approach is employed by Aggarwal in [Agg20b].

1.4 Basic coupling and colored (multispecies) models

Stochastic particle systems we mainly consider in these notes have indistinguishable particles. There exists a systematic way of introducing different species (colors) of particles, such that many of the properties of the systems can be generalized. These colored extensions are related to the so-called *basic coupling* of two (or more) ordinary (monochrome) particle systems. A systematic treatment of colored stochastic vertex models can be found in [BW18]. More precisely, Chapter 2 in this paper introduces the models, and in Chapter 12 one can find various degenerations of the vertex model to particle systems (a story parallel to Sections 1.2.3 and 1.2.4 above). Further properties of colored vertex models such as their symmetries and shift-invariance are explored in [Buf20], [BGW22], [Gal21]. A sample configuration of a colored stochastic six vertex model is given in Figure 4, left.

Here we briefly describe the basic coupling for ASEP and the stochastic six vertex model. Consider two copies of ASEP, $ASEP_1$ and $ASEP_2$, on two copies of $\mathbb{Z}$ which evolve in parallel. Namely, their independent exponential clocks are attached to sites (two clocks per site, of rates 1 and q for right and left jumps, respectively), and are synchronized. If a clock at a site rings, but there is no particle at this site, then nothing happens. Otherwise, each copy of ASEP performs

jumps according to the usual ASEP rules. Here is an illustration of a few possible jumps:

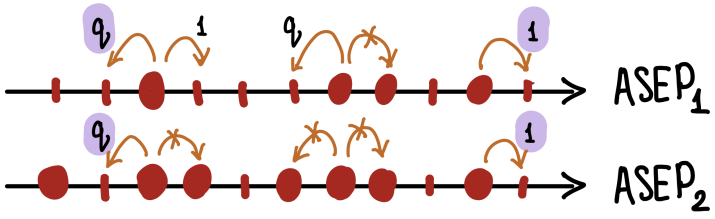

We highlighted the synchronized jumps which must occur simultaneously.

Observe that if at the initial time moment we have $ASEP_2 \geq ASEP_1$, that is, the second configuration contains all the particles from the first configuration (and maybe more particles), then the relation $ASEP_2 \geq ASEP_1$ holds for all times. In this case, let us project the synchronized system of two ASEPs into a single *two-color ASEP* on $\mathbb{Z}$ as follows. If at some $x \in \mathbb{Z}$ there is a particle only in $ASEP_2$, then put particle of color 1 at x. If at x there are particles in both $ASEP_1$ and $ASEP_2$, then put a particle of color 2 at x. Finally, if at x there are holes in both $ASEP_1$ and $ASEP_2$, then put a hole at x. In particular, the above configuration of two ASEPs lead to the following two-color configuration:

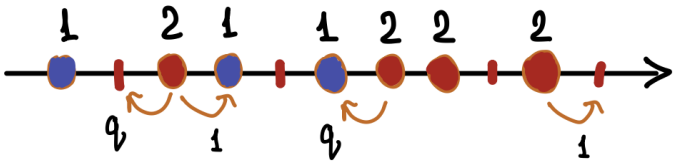

We have also indicated the corresponding jumps.

The basic coupling can be generalized to an arbitrary number of ASEPs, and this leads to a colored ASEP in which colors can take arbitrary integer values. Each adjacent pair of particles of colors (i, j) can exchange into the pair (j, i) at rate q if $i < j$, or at rate 1 if $i > j$. We see that lower colors have less jumping priority if $q < 1$. These jumping rules can also include holes, which we can treat as particles of the lowest color $-\infty$.

The colored ASEP satisfies the *projection property* into the original monochrome ASEP. Namely, take a colored ASEP with colors $\{-\infty, 1, 2, \ldots, n\}$. For a fixed $1 \leq k \leq n$, declare that particles with colors $< k$ are all holes, and with colors $\geq k$ are all single-colored identical particles. Then under this projection we get back the original ASEP. Moreover, if for some $1 \leq k < \ell \leq n$ we identify all particles with colors $k, k+1, \ldots, \ell$, then we get a colored ASEP with fewer colors.

Let us now present the colored stochastic six vertex model without constructing the (now two-dimensional) basic coupling. In the colored stochastic six vertex model, edges can have integer colors. Empty edges may be thought of having the lowest color $-\infty$. The stochastic vertex

weights still depend on two parameters (b_1, b_2), and are as follows:

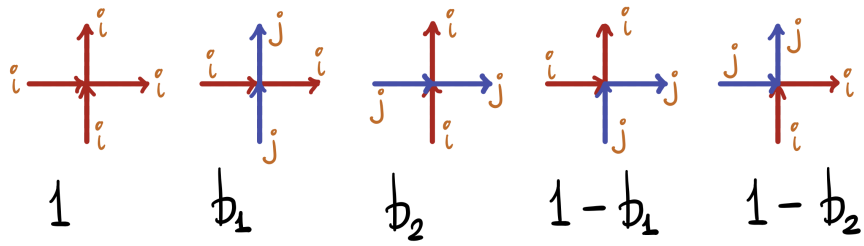

Here we assume that the colors satisfy $i > j$.

In Figure 4, left, there is a sample of the colored stochastic six vertex model in the quadrant $\mathbb{Z}^2_{\geq 0}$ with infinite domain wall boundary conditions. The entering color through the left edge at the horizontal y has color y. That is, the lower entering colors (which are closer to the violet end of the spectrum) have less priority. Figure 4, we identified all colors from the left figure, and in this way we get a sample of the ordinary (monochrome) stochastic six vertex model. In Figure 4, there is a smaller sample of the latter model.

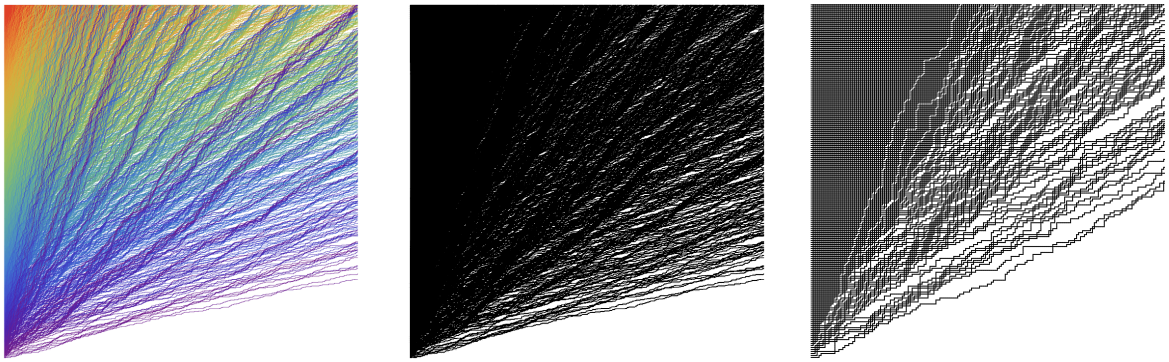

Figure 4: Colored stochastic six vertex model, its monochrome projection, and a smaller simulation of the monochrome six vertex model.

1.5 Stationary distributions and hydrodynamics

The asymptotic limit shape of a stochastic interacting particle system can be obtained via *hydrodynamics*. This allows to write down a partial differential equation for the limiting density based on the analysis of translation invariant distributions of particles which are stationary under the stochastic dynamics.

Let us demonstrate that Bernoulli product measures are invariant for the stochastic six vertex model, and write down the hydrodynamic equation. For a full classification including blocking measures, see [Lin22]. For rigorous hydrodynamics of the stochastic six vertex model, we refer to [Agg20a].

For given b_1, b_2, let us define a function

$$\varphi(\rho) := \frac{\rho(1-b_2)}{1-b_1+b_1\rho-b_2\rho}. \tag{1.9}$$

Take a single vertex of the stochastic six vertex model, and denote by $(i_1, j_1, i_2, j_2) \in \{0,1\}^4$ the numbers of incoming arrows from below and from the left, and the numbers of outgoing arrows from the top and from the right:

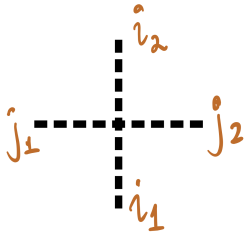

Due to the path preservation property, we have $i_1 + j_1 = i_2 + j_2$, otherwise the vertex weight vanishes.

Proposition 1.13. *Fix $\rho \in [0,1]$. If (i_1, j_1) are random, independent, and distributed as*

$$\mathrm{Prob}(i_1 = 1) = \rho, \qquad \mathrm{Prob}(j_1 = 1) = \varphi(\rho),$$

then (i_2, j_2) are also independent, and distributed as (i_1, j_1).

Proof. The proof is left as an exercise (see Exercise 1.6). □

Exercise 1.6. Prove Proposition 1.13. Hint: consider the probability that the outgoing spin configuration has one outgoing top arrow, and no arrows exiting from the right. We would like this event to have probability $\rho\,(1 - \varphi(\rho))$. Now, compute the same probability by considering two cases for the incoming arrow configuration, and check that they are equal. Finally, repeat this computation for the other outgoing configuration when the single arrow exits from the right and not from the top.

The fact that both computations result in true identities of rational functions of ρ, q, and u, is an indication of the stochastic six vertex model's integrability.

Iterating Proposition 1.13, we obtain the following stationarity of the stochastic six vertex model in the quadrant $\mathbb{Z}^2_{\geq 0}$. Let the configuration of incoming arrows from below be random and distributed as the Bernoulli product measure with density ρ. Let the configuration of incoming arrows from the left be random, independent of the bottom arrows, and have the Bernoulli product distribution with density $\varphi(\rho)$. Then, for any $K, L \geq 0$, the joint distribution of the arrow configuration at the boundary of the shifted quadrant $\mathbb{Z}_{\geq K} \times \mathbb{Z}_{\geq L}$ is the same as for $K, L = 0$. See Figure 5 for an illustration.

This stationarity in the quadrant allows to pass to an infinite-volume Gibbs measure on up-right paths in the full plane, such that the densities of occupied vertical and horizontal edges are ρ and $\varphi(\rho)$, respectively. Namely, shift the origin to the point (K, L), and take a limit as $K, L \to +\infty$. In this limit, we get a consistent family of distributions on growing quadrants, which give rise to the desired infinite-volume Gibbs measure. This Gibbs measure is called the *KPZ pure phase* with density ρ.

Remark 1.14. Naively, the KPZ pure phase describes the distribution of the trajectory of the evolution of the stochastic six vertex model (as a row-to-row Markov chain), when started from the product Bernoulli measure on $\mathbb{Z}$ with density ρ. However, due to the interaction dependence coming from negative infinity, the definition of this evolution is not straightforward, and requires a limit transition with growing quadrants.

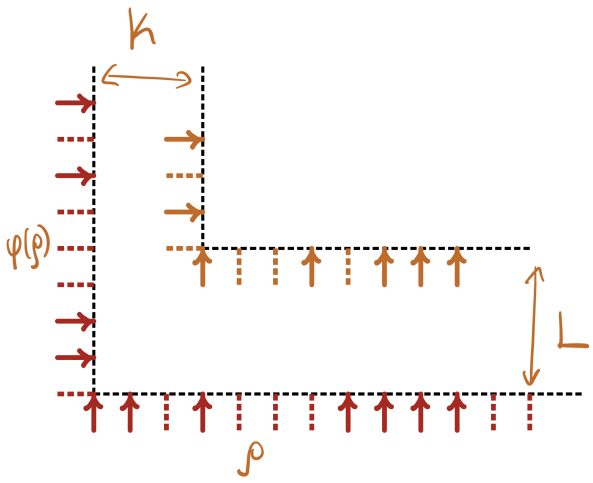

Figure 5: If the joint distribution at the boundary of the original quadrant $\mathbb{Z}^2_{\geq 0}$ is product Bernoulli with density ρ at the bottom and with density $\varphi(\rho)$ on the left, then we have the same joint distribution at the boundary of the shifted quadrant $\mathbb{Z}_{\geq K} \times \mathbb{Z}_{\geq L}$.

By Remark 1.14, we can say that the Bernoulli product measures on $\mathbb{Z}$ are stationarity for the stochastic six vertex on the full line. These stationarity properties can be pushed through the limits of the stochastic six vertex model to particle systems such as ASEP and PushTASEP (Sections 1.2.3 and 1.2.4). Thus, we conclude that the Bernoulli product measures are also stationary for ASEP and PushTASEP. These results were established much earlier, see [Lig76], [Lig05], [Gui97], [AG05] for classifications of stationary measures.

Let us now turn to hydrodynamics. A general principle going back to Onsager [Ons31] in the context of nonequilibrium thermodynamics is that the particle current generated by local stationary distributions affects the global limiting density. Indeed, assume that the stochastic six vertex model starts from an initial configuration which converges to a density profile, for example, in the following way:

$$\rho(\mathsf{x},0)=\lim_{\varepsilon\to 0}\frac{\#\{\text{of vertical arrows in } [\mathsf{x}\varepsilon^{-1}-\varepsilon^{1-\gamma},\mathsf{x}\varepsilon^{-1}+\varepsilon^{1-\gamma}]\}}{2\varepsilon^{1-\gamma}},$$

where $\gamma>0$ is sufficiently small, and $\mathsf{x}\in\mathbb{R}$. Apply the row-to-row Markov transition operator to this initial configuration a large number of times equal to $\mathsf{y}\varepsilon^{-1}$, where $\mathsf{y}\in\mathbb{R}_{>0}$. This leads to a new limiting density $\rho(\mathsf{x},\mathsf{y})$. That is, we view the vertical coordinate y as "time".

On the other hand, the change of $\rho(\mathsf{x},\mathsf{y})$ at a point x during small time interval $d\mathsf{y}$ can occur only due to the difference of the particle currents on both sides of x. From Proposition 1.13 and the subsequent discussion, it follows that the particle current for a Bernoulli product measure of density ρ is equal to $\varphi(\rho)$, where φ is given by (1.9). Thus, the density $\rho(\mathsf{x},\mathsf{y})$ should satisfy the inviscid Burgers like differential equation

$$\frac{\partial}{\partial \mathsf{y}}\rho(\mathsf{x},\mathsf{y})+\frac{\partial}{\partial \mathsf{x}}\varphi\left(\rho(\mathsf{x},\mathsf{y})\right)=0. \tag{1.10}$$

In fact, equation (1.10) does not have a unique solution, and the density function $\rho(\mathsf{x}, \mathsf{y})$ coming from the stochastic six vertex model must be the so-called *entropy solution*. We refer to [Agg20a, Theorem 1.1] for a rigorous derivation of (1.10) from the stochastic six vertex model, and to [Ser99, Section 2.3] for a discussion of entropy solutions to (1.10).

Exercise 1.7. For the infinite domain wall boundary condition, the limiting density

$$\rho(\mathsf{x}, \mathsf{y}) = -\partial_{\mathsf{x}} \mathfrak{h}(\mathsf{x}, \mathsf{y}),$$

where $\mathfrak{h}$ is given by (1.6), can be written down in an explicit form. Write it down, and check that it satisfies the Burgers type equation (1.10).

2 Lecture II. Integrability

3 Lecture III. Asymptotics

References

[ABPW21] A. Aggarwal, A. Borodin, L. Petrov, and M. Wheeler, *Free Fermion Six Vertex Model: Symmetric Functions and Random Domino Tilings*, arXiv preprint (2021). arXiv:2109.06718 [math.PR]. To appear in Selecta Math. ↑5

[AESW51] M. Aissen, A. Edrei, I. J. Schoenberg, and A. Whitney, *On the generating functions of totally positive sequences*, Proc. Nat. Acad. Sci. U. S. A. **37** (1951), 303–307. ↑4

[AG05] E. Andjel and H. Guiol, *Long-range exclusion processes, generator and invariant measures*, Ann. Probab. **33** (2005), no. 6, 2314–2354. arXiv:math/0411655 [math.PR]. ↑16

[Agg18] A. Aggarwal, *Current Fluctuations of the Stationary ASEP and Six-Vertex Model*, Duke Math J. **167** (2018), no. 2, 269–384. arXiv:1608.04726 [math.PR]. ↑11

[Agg20a] A. Aggarwal, *Limit shapes and local statistics for the stochastic six-vertex model*, Commun. Math. Phys. **376** (2020), no. 1, 681–746. arXiv:1902.10867 [math.PR]. ↑14, 17

[Agg20b] A. Aggarwal, *Nonexistence and uniqueness for pure states of ferroelectric six-vertex models*, arXiv preprint (2020). arXiv:2004.13272 [math.PR]. ↑12

[ASLW+15] G. Algara-Siller, O. Lehtinen, F. C. Wang, R. R. Nair, U. Kaiser, H. A. Wu, A. K. Geim, and I. V. Grigorieva, *Square ice in graphene nanocapillaries*, Nature **519** (2015), no. 7544, 443–445. ↑4

[Bax07] R. Baxter, *Exactly solved models in statistical mechanics*, Courier Dover Publications, 2007. ↑4

[BB17] A. Borodin and A. Bufetov, *An irreversible local Markov chain that preserves the six vertex model on a torus*, Ann. Inst. H. Poincaré B **53** (2017), no. 1, 451–463. arXiv:1509.05070 [math-ph]. ↑11

[BBW16] A. Borodin, A. Bufetov, and M. Wheeler, *Between the stochastic six vertex model and hall-littlewood processes*, arXiv preprint (2016). arXiv:1611.09486 [math.PR]. To appear in Jour. Comb. Th. A. ↑10

[BCG16] A. Borodin, I. Corwin, and V. Gorin, *Stochastic six-vertex model*, Duke J. Math. **165** (2016), no. 3, 563–624. arXiv:1407.6729 [math.PR]. ↑7, 8

[BF08] A. Borodin and P. Ferrari, *Large time asymptotics of growth models on space-like paths I: PushASEP*, Electron. J. Probab. **13** (2008), 1380–1418. arXiv:0707.2813 [math-ph]. ↑10

[BGW22] A. Borodin, V. Gorin, and M. Wheeler, *Shift-invariance for vertex models and polymers*, Proceedings of the London Mathematical Society **124** (2022), 182–299. arXiv:1912.02957 [math.PR]. ↑12

[BH20] S. T. Bramwell and M. J. Harris, *The history of spin ice*, Journal of Physics: Condensed Matter **32** (2020), no. 37, 374010. ↑4

[BO12] A. Borodin and G. Olshanski, *The boundary of the Gelfand-Tsetlin graph: A new approach*, Adv. Math. **230** (2012), 1738–1779. arXiv:1109.1412 [math.CO]. ↑4

[Boy83] R. Boyer, *Infinite traces of AF-algebras and characters of $U(\infty)$*, J. Operator Theory **9** (1983), 205–236. ↑4

[Buf20] Alexey Bufetov, *Interacting particle systems and random walks on hecke algebras*, arXiv preprint (2020). arXiv:2003.02730 [math.PR]. ↑12

[BW18] A. Borodin and M. Wheeler, *Coloured stochastic vertex models and their spectral theory*, arXiv preprint (2018). arXiv:1808.01866 [math.PR]. ↑12

[Cor12] I. Corwin, *The Kardar-Parisi-Zhang equation and universality class*, Random Matrices Theory Appl. **1** (2012), 1130001. arXiv:1106.1596 [math.PR]. ↑8

[DLSS91] B. Derrida, J. Lebowitz, E. Speer, and H. Spohn, *Dynamics of an anchored Toom interface*, J. Phys. A **24** (1991), no. 20, 4805. ↑10

[DW08] A.B. Dieker and J. Warren, *Determinantal transition kernels for some interacting particles on the line*, Annales de l'Institut Henri Poincaré **44** (2008), no. 6, 1162–1172. arXiv:0707.1843 [math.PR]. ↑10

[Edr53] A. Edrei, *On the generating function of a doubly infinite, totally positive sequence*, Trans. AMS **74** (1953), 367–383. ↑4

[EKLP92] N. Elkies, G. Kuperberg, M. Larsen, and J. Propp, *Alternating-sign matrices and domino tilings*, Jour. Alg. Comb. **1** (1992), no. 2-3, 111–132 and 219–234. ↑5

[For93] P. J. Forrester, *The spectrum edge of random matrix ensembles*, Nuclear Physics B **402** (1993), 709–728. ↑8

[FR19] M. Fahrbach and D. Randall, *Slow Mixing of Glauber Dynamics for the Six-Vertex Model in the Ordered Phases*, Approximation, randomization, and combinatorial optimization. algorithms and techniques (approx/random 2019), 2019, pp. 37:1–37:20. arXiv:1904.01495 [cs.DS]. ↑6

[FS06] P.L. Ferrari and H. Spohn, *Domino tilings and the six-vertex model at its free-fermion point*, Jour. Phys. A **39** (2006), no. 33, 10297. arXiv:cond-mat/0605406 [cond-mat.stat-mech]. ↑5

[Gal21] P. Galashin, *Symmetries of stochastic colored vertex models*, Annals of Probability **49** (2021), no. 5, 2175–2219. arXiv:2003.06330 [math.PR]. ↑12

[Gho17] P. Ghosal, *Hall-Littlewood-PushTASEP and its KPZ limit*, arXiv preprint (2017). arXiv:1701.07308 [math.PR]. ↑10

[Gor21] V. Gorin, *Lectures on random lozenge tilings*, Cambridge Studies in Advanced Mathematics. Cambridge University Press (2021). ↑6

[GS92] L.-H. Gwa and H. Spohn, *Six-vertex model, roughened surfaces, and an asymmetric spin Hamiltonian*, Phys. Rev. Lett. **68** (1992), no. 6, 725–728. ↑7

[Gui97] H. Guiol, *Un résultat pour le processus d'exclusion à longue portée [a result for the long-range exclusion process]*, Annales de l'Institut Henri Poincare (B) Probability and Statistics **33** (1997), no. 4, 387–405. ↑16

[Har78] T. E. Harris, *Additive set-valued Markov processes and graphical methods*, Ann. Probab. **6** (1978), no. 3, 355–378. ↑9

[IMS21] T. Imamura, K. Mallick, and T. Sasamoto, *Distribution of a Tagged Particle Position in the One-Dimensional Symmetric Simple Exclusion Process with Two-Sided Bernoulli Initial Condition*, Comm. Math. Phys. **384** (2021), 1409–1444. ↑8

[Kas61] P. W. Kasteleyn, *The statistics of dimers on a lattice: I. The number of dimer arrangements on a quadratic lattice*, Physica **27** (1961), no. 12, 1209–1225. ↑3

[KOS06] R. Kenyon, A. Okounkov, and S. Sheffield, *Dimers and amoebae*, Ann. Math. **163** (2006), 1019–1056. arXiv:math-ph/0311005. ↑4

[KPZ86] M. Kardar, G. Parisi, and Y. Zhang, *Dynamic scaling of growing interfaces*, Physical Review Letters **56** (1986), no. 9, 889. ↑8

[Kup96] G. Kuperberg, *Another proof of the alternative-sign matrix conjecture*, Intern. Math. Research Notices **1996** (1996), no. 3, 139–150. ↑6

[Lie67] E.H. Lieb, *Residual entropy of square ice*, Physical Review **162** (1967), no. 1, 162–172. ↑4

[Lig05] T. Liggett, *Interacting Particle Systems*, Springer-Verlag, Berlin, 2005. ↑7, 16

[Lig76] T. Liggett, *Coupling the simple exclusion process*, Ann. Probab. (1976), 339–356. ↑16

[Lin22] Y. Lin, *Classification of stationary distributions for the stochastic vertex models*, arXiv preprint (2022). arXiv:2205.10654 [math.PR]. ↑14

[MG69] C. MacDonald and J. Gibbs, *Concerning the kinetics of polypeptide synthesis on polyribosomes*, Biopolymers **7** (1969), no. 5, 707–725. ↑9

[MGP68] C. MacDonald, J. Gibbs, and A. Pipkin, *Kinetics of biopolymerization on nucleic acid templates*, Biopolymers **6** (1968), no. 1, 1–25. ↑9

[Nap23] S. Naprienko, *Free Fermionic Schur Functions*, arXiv preprint (2023). arXiv:2301.12110. ↑5

[Ons31] L. Onsager, *Reciprocal Relations in Irreversible Processes. I.*, Phys. Rev. **37** (1931), 405. ↑16

[Pau35] L. Pauling, *The structure and entropy of ice and of other crystals with some randomness of atomic arrangement*, Journal of the American Chemical Society **57** (1935), no. 12, 2680–2684. ↑4

[Pet14] L. Petrov, *The Boundary of the Gelfand-Tsetlin Graph: New Proof of Borodin-Olshanski's Formula, and its q-analogue*, Mosc. Math. J. **14** (2014), no. 1, 121–160, available at 1208.3443. arXiv:1208.3443 [math.CO]. ↑4

[Pro01] J. Propp, *The many faces of alternating-sign matrices*, Discrete Mathematics and Theoretical Computer Science (2001). arXiv:math/0208125 [math.CO]. ↑6

[Res10] N. Reshetikhin, *Lectures on the integrability of the 6-vertex model*, Exact Methods in Low-dimensional Statistical Physics and Quantum Computing, 2010, pp. 197–266. arXiv:1010.5031 [math-ph]. ↑3, 4

[Ser99] D. Serre, *Systems of Conservation Laws. 1. Hyperbolicity, Entropies, Shock Waves*, translated by I. N. Sneddon, Cambridge University Press, Cambridge, 1999. Translated From the 1996 French Original. ↑17

[She05] S. Sheffield, *Random surfaces*, Astérisque **304** (2005). arXiv:math/0304049 [math.PR]. ↑4

[Spi70] F. Spitzer, *Interaction of Markov processes*, Adv. Math. **5** (1970), no. 2, 246–290. ↑9, 10

[TF61] H. Temperley and M. Fisher, *Dimer problem in statistical mechanics - an exact result*, Philos. Mag. **6** (1961), no. 68, 1061–1063. ↑3

[TW08] C. Tracy and H. Widom, *Integral formulas for the asymmetric simple exclusion process*, Comm. Math. Phys **279** (2008), 815–844. arXiv:0704.2633 [math.PR]. Erratum: Commun. Math. Phys., 304:875–878, 2011. ↑7

[TW09] C. Tracy and H. Widom, *Asymptotics in ASEP with step initial condition*, Commun. Math. Phys. **290** (2009), 129–154. arXiv:0807.1713 [math.PR]. ↑7

[TW94] C. Tracy and H. Widom, *Level-spacing distributions and the Airy kernel*, Commun. Math. Phys. **159** (1994), no. 1, 151–174. arXiv:hep-th/9211141. ↑8

[VK82] A. Vershik and S. Kerov, *Characters and factor-representations of the infinite unitary group*, Dokl. Akad. Nauk SSSR **267** (1982), no. 2, 272–276. ↑4

[Voi76] D. Voiculescu, *Representations factorielles de type II_1 de $U(\infty)$*, J. Math. Pures Appl. **55** (1976), 1–20. ↑4

[YY66] C.N. Yang and C.P. Yang, *One dimensional chain of anisotropic spin-spin interaction*, Phys. Rev. (1966), 150: 321–327, 327–339; 151: 258–264. ↑4

[ZJ00] Paul Zinn-Justin, *Six-vertex model with domain wall boundary conditions and one-matrix model*, Phys. Rev. E **62** (2000), no. 3, 3411. arXiv:math-ph/0005008. ↑5

University of Virginia, Charlottesville, VA
E-mail: lenia.petrov@gmail.com